First published in:

Negative beam displacements from negative-index photonic metamaterials

G. Dolling[1], **M. W. Klein**[1], **M. Wegener**[1], **A. Schädle**[2],
B. Kettner[2], **S. Burger**[2], **and S. Linden**[3*]

[1]*Institut für Angewandte Physik and DFG-Center for Functional Nanostructures (CFN),*
Universität Karlsruhe (TH), Wolfgang-Gaede-Str. 1, D-76128 Karlsruhe, Germany
[2]*Zuse Institute Berlin and DFG Forschungszentrum Matheon,*
Takustr. 7, D-14195 Berlin, Germany
[3]*Institut für Nanotechnologie, Forschungszentrum Karlsruhe in der Helmholtz-Gemeinschaft,*
Postfach 3640, D-76021 Karlsruhe, Germany
[*]*Corresponding author: Stefan.Linden@physik.uni-karlsruhe.de*

Abstract: It is well known that refraction of light at interfaces leads to a beam displacement for oblique incidence of light onto a slab of material. In ray optics and for homogeneous isotropic materials, the sign of this beam displacement is strictly identical to the sign of the refractive index. Our numerical calculations reveal negative beam displacements from state-of-the-art double-fishnet-type photonic metamaterials. This holds true for the "main" polarization corresponding to a negative phase velocity for normal incidence as well as for the "secondary" polarization with positive phase velocity. To understand and interpret these results, we also present exact analytical calculations for thin metal films showing that, in wave optics, the sign of the beam displacement (i.e., the sign of refraction) is generally not identical to the sign of the refractive index.

© 2007 Optical Society of America

OCIS codes: (160.4760) Optical properties; (260.5740) Resonance; (999.9999) Metamaterials

References and links

1. V. G. Veselago, "The electrodynamics of substances with simultaneuously negative values of ε and μ," Sov. Phys. Uspekhi **10**, 509–514 (1968).
2. V. M. Shalaev, "Optical negative-index metamaterials," Nature Photon. **1**, 41–48 (2006).
3. C. M. Soukoulis, S. Linden, and M. Wegener, "Negative Refractive Index at Optical Wavelengths," Science **315**, 47–49 (2007).
4. K. Busch, G. von Freymann, S. Linden, S. Mingaleev, L. Tkeshelashvili, and M. Wegener, "Periodic nanostructures for photonics," Phys. Rep. **444**, 101–202 (2007).
5. R. A. Shelby, D. R. Smith, and S. Schultz, "Experimental Verfication of a Negative Index of Refraction," Science **292**, 77–79 (2001).
6. G. Dolling, M. Wegener, and S. Linden, "Realization of a three-functional-layer negative-index photonic metamaterial," Opt. Lett. **32**, 551–553 (2007).
7. G. Dolling, C. Enkrich, M. Wegener, C. M. Soukoulis, and S. Linden, "Simultaneous Negative Phase and Group Velocity of Light in a Metamaterial," Science **312**, 892–894 (2006).
8. G. Dolling, C. Enkrich, M. Wegener, C. M. Soukoulis, and S. Linden, "Low-loss negative-index metamaterial at telecommunication wavelengths," Opt. Lett. **31**, 1800–1802 (2006).
9. G. Dolling, M. Wegener, C. M. Soukoulis, and S. Linden, "Negative-index metamaterial at 780 nm wavelength," Opt. Lett. **32**, 53–55 (2007).
10. X. L. Chen, M. He, Y. Du, W. Y. Wang, and D. F. Zhang, "Negative refraction: An intrinsic property of uniaxial crystals," Phys. Rev. B **72**, 113111 (2005).
11. E. Shamonina and L. Solymar, "Properties of magnetically coupled metamaterial elements," J. Magn. Magn. Mater. **300**, 38-43 (2006).

12. G. Dolling, M. Wegener, A. Schädle, S. Burger, and S. Linden, "Observation of magnetization waves in negative-index photonic metamaterials," Appl. Phys. Lett. **89**, 231118 (2006).
13. F. Goos and H. Hänchen, "Ein neuer und fundamentaler Versuch zur Totalreflexion," Ann. Physik **1**, 333–346 (1947).
14. F. Goos and H. Hänchen, "Neumessung des Strahlversetzungseffektes bei Totalreflexion," Ann. Physik **5**, 251–252 (1949).
15. H. M. Lai, C. W. Kwok, Y. W. Loo, and B. Y. Xu, "Energy-flux pattern in the Goos-Hänchen effect," Phys. Rev. E **62**, 7330–7339 (2000).
16. S. Zhang, W. Fan, K. J. Malloy, S. R. Brueck, N. C. Panoiu, and R. M. Osgood, "Near-infrared double negative metamaterials," Opt. Express **13**, 4922–4930 (2005).
17. S. Burger, R. Klose, A. Schädle, F. Schmidt, and L. Zschiedrich, "FEM modelling of 3D photonic crystals and photonic crystal waveguides," Proc. SPIE Vol. **5728**, 164–173 (2005).
18. L. Zschiedrich, R. Klose, A. Schädle, and F. Schmidt, "A new finite element realization of the Perfectly Matched Layer Method for Helmholtz scattering problems on polygonal domains in 2D," J. Comput Appl. Math., **188**, 12–32 (2006).
19. L. Zschiedrich, S. Burger, B. Kettner, and F. Schmidt, "Advanced Finite Element Method for Nano-Resonators," Proc. SPIE Vol. **6115**, 164–174 (2006).
20. P. B. Johnson and R. W. Christy, "Optical Constants of the Noble Metals," Phys. Rev. B **6**, 4370–4379 (1972).
21. E. Hecht, *Optics* (Addison Wesley, 2001).
22. J. B. Pendry, "Negative Refraction Makes a Perfect Lens," Phys. Rev. Lett. **85**, 3966–3969 (2000).
23. M. Wegener, G. Dolling, and S. Linden, "Backward waves moving forward," Nature Mater. **6**, 475–476 (2007).

1. Introduction

All known natural substances exhibit a negligible magnetic response at optical frequencies, i.e., their magnetic permeability μ is equal to one. Thus, optics & photonics have solely been controlling directly the electric component of the electromagnetic light wave and not the magnetic component – obviously limiting the opportunities regarding the control of light. Photonic metamaterials are man-made artificial materials composed of functional sub-wavelength building blocks that are densely packed into an effective material. Such metamaterials can reveal both, an electric as well as a magnetic response, which can lead to a negative index of refraction in the spirit of the work of Veselago [1]. Recent reviews on photonic metamaterials can be found in Refs. [2, 3, 4].

At microwave frequencies, negative refraction has directly been measured by using a prism geometry [5]. At optical frequencies, presently available negative-index photonic metamaterials are thin films [2, 3, 4], usually composed of just a single monolayer with one notable exception [6]. This fact has inhibited experiments addressing the aspect of refraction, i.e., a change of the propagation direction of the Poynting vector of light at an interface. The negative refractive index has rather been addressed by measuring the negative time-of-flight connected with the negative phase velocity of light [7, 8, 9]. Furthermore, presently available negative-index metamaterials operating at optical frequencies are polarization dependent for normal incidence and they are highly anisotropic for oblique incidence of light. These aspects can lead to negative refraction [10], even for positive phase velocities. Moreover, the coupling among the different building blocks leads to magnetization waves (or magneto-inductive waves) [11], which have recently been observed experimentally [12] at optical frequencies for oblique incidence of light and which can alternatively be cast into spatial dispersion of the effective permittivity and permeability. This means that these quantities are not only frequency-dependent but also dependent on the wave vector of light. In other words, the electromagnetic material response becomes non-local in real space. This aspect can lead to the so-called additional-boundary-condition problem – unless the material response is treated microscopically. Thus, altogether, it is not clear, whether such photonic metamaterials would exhibit negative refraction for oblique incidence of light at all.

As prism geometries appear to be out of reach for the near future in the present context, we consider the beam displacement Δx that occurs when a beam of light passes through a slab of
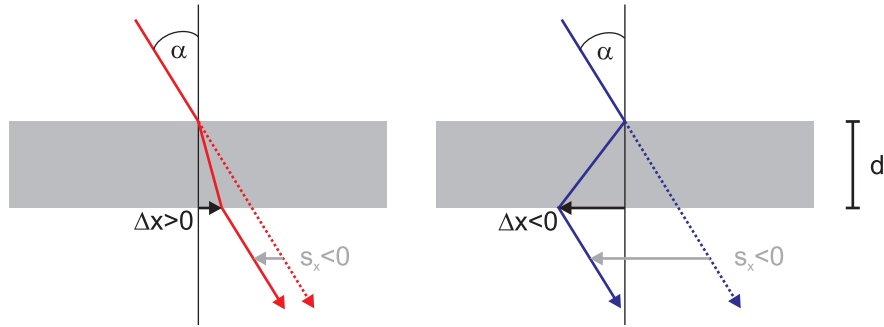
Fig. 1. Light impinges from vacuum onto a slab (gray area) of an isotropic and homogeneous material of thickness d under oblique incidence with an angle α as indicated. In ray optics, a positive real part of the refractive index $\mathrm{Re}(n) > 0$ leads to a positive beam displacement $\Delta x > 0$ (left panel), whereas the displacement is negative (right panel) for a negative refractive index $\mathrm{Re}(n) < 0$. The shift of the transmitted beam, s_x, is also indicated.

material. The geometry is schematically defined in Fig. 1. It is clear that, in ray optics and for a homogeneous isotropic material with complex refractive index n, the beam displacement is positive for $\mathrm{Re}(n) > 0$ and negative for $\mathrm{Re}(n) < 0$. The order of magnitude of this displacement is very roughly given by the thickness d of the slab. Thus, presently available photonic metamaterials with thicknesses on the order of 100 nm will lead to sub-wavelength beam displacements. In an actual experiment, one could directly measure the shift s_x in that plane along the x-direction between "sample out" and "sample in (vacuum)". This quantity s_x is also directly computed in the numerical calculations. From basic trigonometry, the displacement Δx (see Fig. 1) results as $\Delta x = d \tan(\alpha) + s_x$. This definition deserves some discussion. While s_x could be an actual observable, Δx will likely not. Nevertheless, we will depict Δx rather than s_x in the following figures because Δx has an intuitive meaning in ray optics. In wave optics, one has to be a little cautious with the interpretation of this Δx. It can be interpreted as the shift along the x-direction between the maximum of the beam profile (e.g., a Gaussian) at the rear side of the sample with respect to the maximum of the incident beam at the front side of the sample. Due to the Goos-Hänchen effect [13, 14, 15], the maximum of the incident beam profile at the front side of the sample does not necessarily coincide with the maximum of the total intensity profile at the front side of the sample.

In the present paper, we start by discussing numerical calculations of the beam displacements from negative-index photonic metamaterials on the basis of the Maxwell equations (i.e., wave optics) for typical parameters corresponding to recent experiments based on the so-called double-fishnet design [16]. Negative beam displacements are found for conditions where the real part of the index of refraction is negative for normal incidence – as might have been expected qualitatively. Quantitatively, however, these finding cannot be explained by the effective parameters obtained from normal incidence. In addition, we also find negative beam displacements for the polarization configuration that corresponds to a diluted metal response (i.e., no negative real part of the refractive index for normal incidence). To better understand this unexpected feature, we also present exact analytical transfer-matrix calculations on the beam displacement from thin silver metal films. As a test, these analytical results are compared with numerical calculations, leading to excellent agreement.

2. Microscopic numerical calculations

All of the following calculations of beam displacements are based on calculations for plane waves impinging from vacuum onto a slab of material under oblique incidence of light. The wave vector of the incident light includes an angle α with the surface normal. In order to define a transverse spatial profile on the front surface of the sample, we consider the interference of N plane waves with incident angles $\alpha_i = \alpha + \delta \frac{i}{N}$, with $i = -(N-1)/2, \ldots, 0, \ldots, +(N-1)/2$ for odd N ($i = -N/2, \ldots, -1, 1, \ldots, +N/2$ for even N). For $N = 2$, this simply leads to a cosine squared intensity pattern, the period of which depends on the "opening angle" δ. Propagation of light through the sample then leads to a displaced pattern on the back side of the sample. It is important to note that we have carefully checked that the resulting Δx does *not* depend on the choice of δ, even if this opening angle is varied over orders of magnitude from values ranging from 0.01 to 10 degrees. Also, we have carefully checked that the obtained displacements Δx do *not* change significantly if five plane waves ($N = 5$) are considered ($N = 3$ is actually shown in this article). In the analytical calculations (see next section), we have even used values up to $N = 500$, mimicking a Gaussian transverse beam profile, without significant changes of Δx. We can conclude that the calculated displacements Δx are a function of the sample (hence, of the wavelength and the polarization of light) and the angle of incidence α, but neither a function of the opening angle nor of the shape of the intensity profile for the conditions considered in this paper.

To calculate the response of each of the individual plane waves under oblique incidence of light, we proceed as previously [12]: We obtain numerically exact solutions of the complete vector Maxwell equations using the advanced finite-element frequency-domain based software package JCMsuite. Bloch-periodic boundary conditions are applied in the x- and y-directions [17] to allow for oblique incidence of light. In the $\pm z$-direction we apply transparent boundary conditions based on the adaptive perfectly-matched-layer (PML) method [18, 19]. We discretize a unit cell with an unstructured mesh of 1 500 to 1 800 prisms, such that the number of points per wavelength is roughly constant. Maxwell's equations are discretized using vectorial finite elements (Whitney elements) of second polynomial order. Together with the adaptive PML, this leads to sparse linear systems with 200 000 to 300 000 unknowns. This problem is solved using *PARDISO*, which is provided by Intel's Math Kernel Library.

We have performed systematic calculations of beam displacements for three different parameter sets for double-fishnet negative-index photonic metamaterials corresponding to the three Refs. [7, 8, 9]. The overall qualitative behavior is found to be rather similar. Thus, we here only show results for one of them [7]. In that work, it has been shown explicitly by means of normal-incidence interferometric pulse propagation experiments that the phase velocity of light is negative at around $1.5\,\mu$m wavelength and for an incident electric-field vector parallel to the thin wires. In contrast, for the orthogonal linear incident polarization, the behavior of a diluted Drude metal has been found, which means that the phase velocity of light is positive for the entire spectral range. Furthermore, we have presented a systematic study of transmittance spectra under oblique incidence for a closely similar (but not identical) sample in Ref. [12]. In this fashion, we can avoid too much repetition here. For convenience of the reader, the structure under investigation is depicted in Fig. 2. Its physics has extensively been reviewed in Ref. [4]. The parameters used in the present work are identical to those used in the calculations of Ref. [7], i.e., $t = 25\,$nm, $s = 35\,$nm, $w_x = 307\,$nm, $w_y = 100\,$nm. These elements are arranged on a square lattice with lattice constant $a_x = a_y = a = 600\,$nm. The metamaterial thickness results as $d = 2t + s = 85\,$nm. For the description of the gold, we employ the Drude model with a plasma frequency $\omega_{pl} = 1.32 \cdot 10^{16}\,$s^{-1} and a collision frequency $\omega_{col} = 1.2 \cdot 10^{14}\,$s^{-1}. The refractive index of the MgF$_2$ is taken as $n = 1.38$, that of the glass substrate as $n = 1.5$.

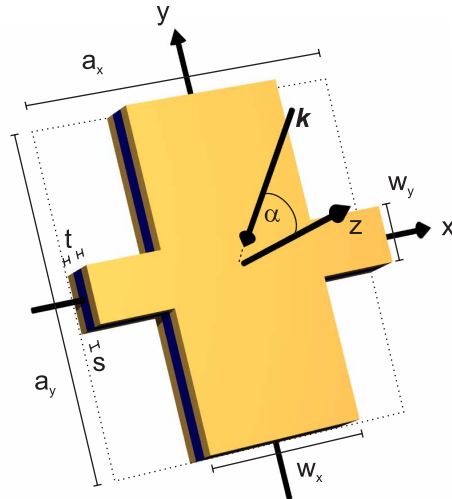Fig. 3 gives an overview of the obtained results. The spectral range is chosen to match that

Fig. 2. Illustration of one unit cell of a single layer of the well-known so-called double-fishnet design of negative-index photonic metamaterials. The parameters are indicated. The yellow regions are the metal (Au), the blue region is the dielectric spacer (MgF$_2$). The structure is located on a glass substrate (not shown).

of Fig. 4 of Ref. [7] for convenience of the reader. Fig. 3(a) shows the calculated transmittance spectra for angles of incidence $\alpha = 0, 10, 20$ and 30 degrees as indicated (compare Ref. [12]) and for the two orthogonal incident linear polarizations (also see inset). The "main" polarization (electric-field vector parallel to the thin wires), which exhibits a region with $\mathrm{Re}(n) < 0$, corresponds to the solid curves, the orthogonal "secondary" polarization to the dashed curves. Here, as usual, n is defined via $n^2 = \varepsilon\mu$. The retrieved [4, 7] $\mathrm{Re}(n)$ and $\mathrm{Im}(n)$ are depicted in Fig. 3(b), showing $\mathrm{Re}(n) < 0$ for the main polarization. The beam displacements Δx, calculated along the above lines, are shown in Fig. 3(c). For the main polarization, the spectral profiles of $\mathrm{Re}(n)$ and Δx roughly match in the sense that negative beam displacements $\Delta x < 0$ occur where we find $\mathrm{Re}(n) < 0$ for normal-incidence. At first sight, this observation appears to suggest that one could simply have introduced $\mathrm{Re}(n)$ into Snell's law. Two facts, however, show that the behavior is more complex. (i) First, we also find negative beam displacements for the "secondary" incident polarization of light – for which Fig. 3(b) shows $\mathrm{Re}(n) > 0$ throughout the entire relevant spectral range. We will explain this unexpected aspect by exact analytical calculations for a model configuration in the next section. (ii) Second, one can take the permittivity ε and the permeability μ retrieved from normal-incidence [2, 3, 4, 7], assume (against better knowledge) an isotropic material response, and compute the beam displacement of a slab of thickness d on this basis (also see next section). As pointed out above, this approach deliberately ignores all complications such as anisotropy or spatial dispersion. These results are shown in Fig. 3(d). It is obvious that they show little resemblance with the correct results (Fig. 3(c)). Not even the sign of Δx is necessarily correct. Furthermore, large quantitative deviations arise throughout the entire spectral range for both polarizations.

3. Negative beam displacements from metal films

This section serves two purposes. First, it discusses a model geometry that has exact analytical solutions, thus allowing for a test of the purely numerical calculations presented in the preceding section. Second, we aim at clarifying the obtained negative beam displacements $\Delta x < 0$ for
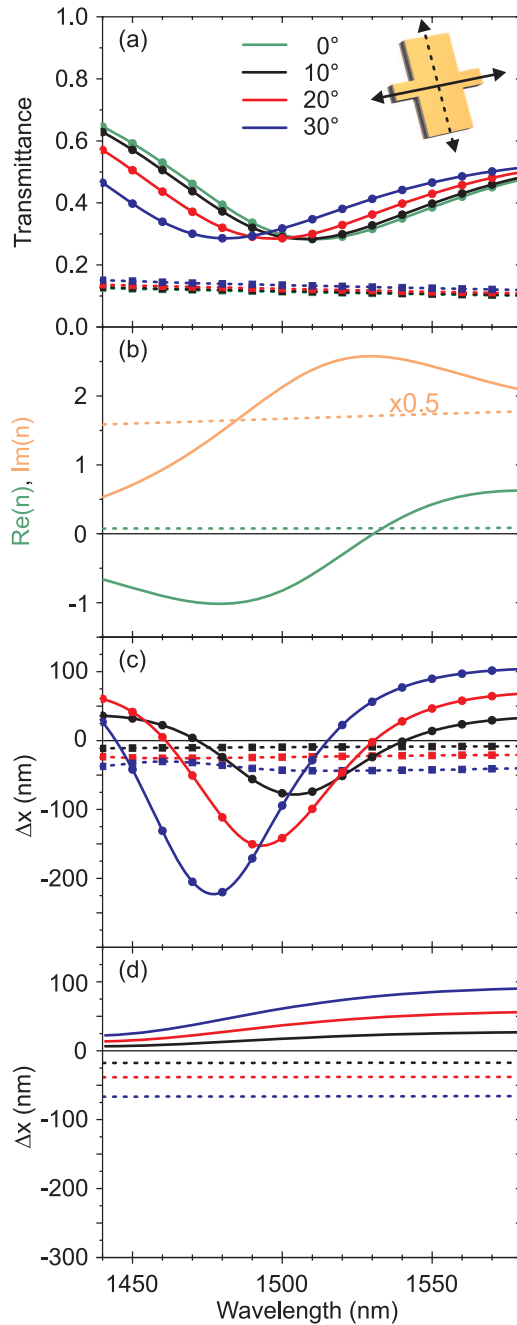
Fig. 3. Calculated response for the sample structure shown in Fig. 2 and for the geometry illustrated in Fig. 1. Results are shown for the "main" polarization (solid) and for the "secondary" polarization (dashed). The configurations are illustrated by the inset. The arrows indicate the polarization, i.e., the orientation of the electric-field vector of the incident light. (a) Intensity transmittance spectra for the angles of incidence as indicated, (b) retrieved values of the complex quantity n for normal incidence, (c) calculated beam displacements Δx for the complete microscopic theory, and (d) Δx obtained from the parameters obtained from the normal-incidence retrieval. The symbols in (a) and (c) are calculated, the curves are guides to the eye.
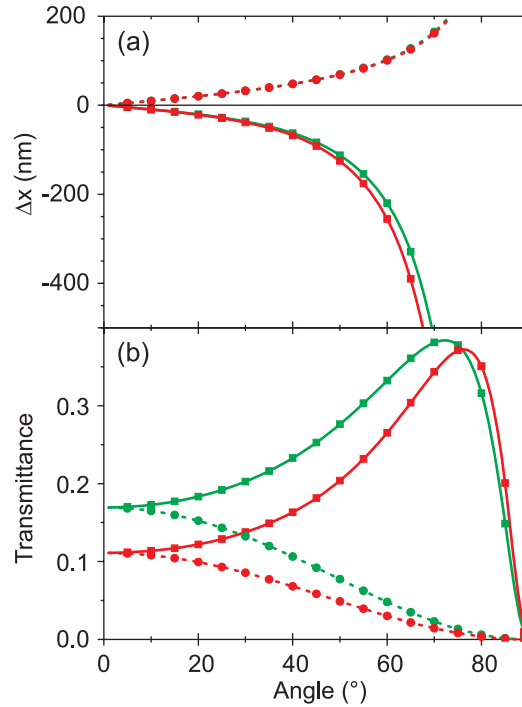
Fig. 4. (a) Beam displacements versus angle of incidence α obtained from exact analytical calculations (curves) and complete numerical calculations (symbols) for p- (solid) and s-polarized (dashed) light, respectively, for oblique incidence onto a free-standing 25-nm thin silver film. The two different incident wavelengths are 532 nm (green curves) and 650 nm (red curves). (b) Corresponding (intensity) transmittance spectra. Note the excellent agreement between analytical and numerical results.

conditions where $\mathrm{Re}(n) > 0$ for the secondary polarization.

We consider a free-standing metal film. Light can impinge under oblique incidence in p-polarization or in s-polarizations. It is clear that this geometry is unlikely to be realized in an experiment, its purpose is solely to provide a conceptually clear gedankenexperiment. (We have also performed corresponding calculations for a metal film on a glass substrate. The results are qualitatively similar but quantitative deviations do occur.) Here, we show results for a $d = 25\,\mathrm{nm}$ thin film of silver using literature permittivity values [20] ($\varepsilon(532\,\mathrm{nm}) = -11.56 + \mathrm{i}0.34$ and $\varepsilon(650\,\mathrm{nm}) = -18.49 + \mathrm{i}0.43$, thus $n(532\,\mathrm{nm}) = 0.05 + \mathrm{i}3.4$ and $n(650\,\mathrm{nm}) = 0.05 + \mathrm{i}4.3$). In the numerics, we proceed as outlined in the last section. Results are shown as the symbols in Fig. 4. Negative beam displacements $\Delta x < 0$ are found for p-polarization of light, which corresponds to the secondary polarization of the photonic metamaterial.

To obtain exact analytical results, we first calculate the response for a single linearly polarized plane wave impinging under oblique incidence using the transfer-matrix approach [21] and then proceed as with the numerical approach for $N = 3$ (see discussion above). For a single plane wave, the known transfer matrix for p-polarization is given by

$$E_\mathrm{t} = \frac{Z_\mathrm{t}}{Z_\mathrm{i}} \frac{2\gamma_\mathrm{t}}{\gamma_\mathrm{i}\cos(kd) - \dfrac{\gamma_\mathrm{i}\gamma_\mathrm{t}}{\gamma_\mathrm{m}}\mathrm{i}\sin(kd) - \gamma_\mathrm{m}\mathrm{i}\sin(kd) + \gamma_\mathrm{t}\cos(kd)} E_\mathrm{i} \qquad (1)$$

and similarly for s-polarization

$$E_t \;=\; \frac{2\gamma_i'}{\gamma_i'\cos(kd) - \dfrac{\gamma_i'\gamma_t'}{\gamma_m'}\,i\sin(kd) - \gamma_m'\,i\sin(kd) + \gamma_t'\cos(kd)}\,E_i. \tag{2}$$

The subscripts are "i" for the medium of incidence, "t" for the medium transmitted into, and "m" for the slab. Z is the impedance, $k = k_0\,n_m\cos(\alpha_m)$ with the vacuum wave vector k_0 and the angle α_m inside the slab with respect to the surface normal, and $n = n_m$ is the complex refractive index of the slab. The quantities $\gamma_j = \left(Z_j\cos(\alpha_j)\right)^{-1}$ and $\gamma_j' = Z_j^{-1}\cos(\alpha_j)$ with $j = i, m, t$ are abbreviations with the angles $\alpha_{i,m,t}$ with respect to the surface normal in the respective medium (with $\alpha_i = \alpha$).

Results are shown as the curves in Fig. 4 which can be compared with the corresponding numerical calculations depicted as the symbols in the same figure. Obviously, the agreement is excellent. This finding gives us confidence that the purely numerical results shown and discussed in the last section are indeed correct.

Numerical and analytical calculations agree in that negative beam displacements $\Delta x < 0$ can occur while the metal real part of the "refractive index" is clearly positive (i.e., $\mathrm{Re}(n) > 0$). This result is related to the negative Goos-Hänchen shifts obtained in calculations for reflection of light from metal half-spaces [15] and it is also closely connected to the "poor man's perfect lens" [22]. This behavior results from antiparallel tangential components of the Poynting vector $\vec{S}$ and the wave vector of light $\vec{k}$ that occur inside the metal for p-polarization of light, leading to $\vec{k}\cdot\vec{S} < 0$. Waves with $\vec{k}\cdot\vec{S} < 0$ are generally known as backward waves. In s-polarization, no backward waves are excited.

Let us briefly recall the underlying physics: While the tangential component of the wave vector of light $\vec{k}$ is conserved at the air/metal interface (and, hence, the tangential component of the phase velocity of light keeps its sign), the tangential component of the Poynting vector $\vec{S} = \vec{E} \times \vec{H}$ changes sign for p-polarization because the normal component of the $\vec{E}$-field jumps discontinuously at the interface and changes sign as a result of the negative metal permittivity ε, whereas the tangential component of the $\vec{H}$-field is conserved according to Maxwell's equations. In s-polarization no backward waves occur because the electric field has zero component normal to the metal interface in this case. The backward wave inside the metal for p-polarization corresponds to negative refraction in the usual meaning. On the other side of the metal film, again negative refraction occurs (see Fig. 1). The net result is a wave which has a wave vector that is parallel to the incident one and which is displaced by $\Delta x < 0$ (Fig. 1) – despite the fact that $\mathrm{Re}(n) > 0$ (with $n = \sqrt{\varepsilon}$) for the isotropic and homogeneous metal film.

Clearly, the metal indeed leads to significant reflection and losses, but these are even comparable to those of negative-index photonic metamaterials [2, 3]. Corresponding transmittance spectra are shown in Fig. 4(b). It becomes evident that the transmittance lies above 30% for p-polarization, for green light, and for angles of 60 degrees where the beam displacement is as large as $\Delta x \approx -225\,\mathrm{nm}$, the modulus of which is nearly one order of magnitude larger than the metal film thickness $d = 25\,\mathrm{nm}$. Negative beam displacements for p-polarization are also found at longer wavelengths, e.g., for $1.5\,\mu\mathrm{m}$, as well as for thicker silver films, e.g., for $d = 50\,\mathrm{nm}$ (not shown). Clearly, the transmittance decreases for longer wavelengths and/or thicker films.

The results of this section cannot be understood on the basis of Snell's law, which predicts positive beam displacements for metal films – independent of the polarization.

4. Conclusions

In conclusion, we have studied the beam displacement of a light wave impinging onto a slab of a metamaterial under oblique incidence of light by numerical calculations. We have used pa-

rameters that correspond to those of presently available negative-index photonic metamaterials operating at optical frequencies. This gedankenexperiment addresses refraction in the original meaning of the word, i.e., it addresses the modified direction of the flow of electromagnetic energy (the Poynting vector) inside the metamaterial, whereas previous work has focused on the negative phase velocity of light (negative wave vector of light) for normal incidence. Clearly, these two aspects are fundamentally different – despite the fact that they are often both described by *the* refractive index. We find negative beam displacements in wavelength regions where the phase velocity is negative as well as under conditions where the phase velocity is positive.

Furthermore, we have discussed the same displacement geometry for a plain metal film. Here, analytical calculations based on a transfer-matrix approach are in excellent agreement with numerical calculations. This simple but instructive model highlights the difference between the two mentioned aspects. In the case of a simple metal film, negative beam displacements indicative for negative refraction can occur for p-polarization of the incident light (due to backward waves in the metal), while the refractive index defined by $c = c_0/\mathrm{Re}(n)$ and, hence, the phase velocity of light c are positive: Negative refraction occurs for a positive refractive index of a homogeneous and isotropic medium. Thus, we should rather call the quantity $n = \sqrt{\varepsilon}$ (which is often referred to as the refractive index) "the slowness factor of light", and the quantity occurring in Snell's law "the refractive index" [23]. The former describes the wave vector (or the phase velocity) of light, the latter the Poynting vector (or the energy velocity) of light.

Acknowledgements